

Color Image Segmentation Based on Homogram Thresholding and Region Merging

H. D. Cheng, X. H. Jiang and Jingli Wang
Dept. of Computer Science
Utah State University
Logan, UT 84322-4205

Abstract

In this paper, a color image segmentation approach based on homogram thresholding and region merging is presented. The homogram considers both the occurrence of the gray levels and the neighboring homogeneity value among pixels. Therefore, it employs both the local and global information. Fuzzy entropy is utilized as a tool to perform homogram analysis for finding all major homogeneous regions at the first stage. Then region merging process is carried out based on color similarity among these regions to avoid oversegmentation. The proposed homogram-based approach (HOB) is compared with the histogram-based approach (HIB). The experimental results demonstrate that the HOB can find homogeneous regions more effectively than HIB does, and can solve the problem of discriminating shading in color images to some extent.

Keywords

Homogeneity, Color image segmentation, Fuzzy logic, Region merge, Color space, Thresholding.

1 INTRODUCTION

Image segmentation is the first step in image analysis and pattern recognition. It is a critical and essential component of an image analysis and/or pattern recognition system, and is one of the most difficult tasks in image processing, which determines the quality of the final result of analysis.

Color image segmentation attracts more and more attention. It has long been recognized that the human eye can discern thousands of color shades and intensities but only two-dozen shades of gray. The situation often occurs when the objects cannot be extracted using gray scale information but can be extracted using color information. Compared to gray scale, color provides additional information to intensity. People realize that color is useful or even necessary for pattern recognition and computer vision. Also the acquisition and processing hardware for color image become more and more available for dealing with the problem of computation complexity caused by the high-dimensional color space. Hence, color image processing becomes increasingly prevalent nowadays.

In most of the existing color image segmentation approaches, the definition of a region is based on similar color. Monochrome image segmentation techniques can be extended to color image, such as histogram thresholding, clustering, region growing, edge detection, fuzzy logic and neural networks, by using RGB or their transformations (linear/non-linear) as shown in Fig. 1 [1].

Monochrome segmentation methods can be directly applied to each component of a color space, then the results can be combined in some way to obtain the final segmentation results [2]. Generally speaking, monochrome image segmentation approaches are based on either discontinuity and/or homogeneity of gray level values in a region. The approach based on discontinuity tends to partition an image by detecting isolated points, lines and edges based on abrupt changes in gray levels. The approaches based on homogeneity include thresholding, clustering, region growing, and region splitting and merging, etc.

A combination of these approaches is often utilized for color image segmentation [3 - 14]. There are several survey papers on monochrome image segmentation [15 - 20], which cover major image segmentation techniques available.

Each color representation has its advantages and disadvantages. There is still no color representation that can dominate the others for all kinds of color images yet. Nonlinear color transformations such as HSI and normalized color space have essential singularities which are non-removable, and there are spurious modes in the distribution of values resulting from the nonlinear transformations. The major problem of linear color spaces is the high correlation of the three components, which makes the three components dependent upon each other and associate strongly with intensity. Hence, linear spaces are very difficult to discriminate highlights, shadows and shading in color images. Using HSI can solve this problem to some extent except that hue is unstable at low saturation [21].

In this paper, a color image segmentation approach based on *homogram* thresholding and region merging in a color space is presented. The concept of the *homogram* was discussed in [22], which is used to express the information of homogeneous properties among pixels in an image. First, we use homogram analysis to find all major homogeneous regions. Then, the region merging process is carried out based on color similarity among these regions to solve the problem of oversegmentation.

In the subsequent sections, we describes the proposed method in Section 2. The experimental results and discussions are in Section 3. Finally, conclusions are presented in Section 4.

2 PROPOSED METHOD

Histogram thresholding is one of the widely used techniques for monochrome image segmentation [24], but it is based on only gray level and does not take into account the

spatial information of pixels with respect to each other. [22] proposed a fuzzy homogeneity approach to overcome this drawback. The concept of *homogram* was defined to express the information of homogeneous properties among pixels in an image. In this paper, we employ the concept of the homogram to extract homogeneous regions in a color image. The proposed method is divided into two stages. At the first stage, fuzzy homogeneity approach is applied to three color components to find thresholds for each color component, then the segmentation results for the three color components are combined to partition the color space into several clusters. Some of these clusters may only contain too few pixels and should not be considered as proper clusters. Also there might be some clusters that are very close to each other, and they should be merged. This problem will be solved at the second stage using the region merging approach.

2.1 Homogram Thresholding Approach

2.1.1 Homogram

A general concept of the *homogram* is given in [22]. First, *fuzzy homogeneity vector*, which sums the degree of homogeneity occurring between the pixel with gray level t and its neighbors with different angle θ and neighboring distance d , is defined as

$$\begin{aligned}
 h(t, \theta, d) = & \{ \sum \delta_z(|t - r|) \mid t = g(i, j), r = g(k, l), \\
 & t, r \in G, 1 \leq i \leq M, 1 \leq j \leq N, [(i, j), (k, l)] \in (X \times Y) \\
 & \times (X \times Y) \mid |(i, j) - (k, l)| = d \text{ along the } \theta \text{ direction} \}
 \end{aligned} \tag{1}$$

where $\theta \in \{0^\circ, 45^\circ, 90^\circ, 135^\circ, 180^\circ, 225^\circ, 270^\circ, 315^\circ\}$, G is the set of gray levels, and $\delta_z(\cdot)$ is a Z -function, defined as:

$$\delta_z(x) = Z(x, a, b, c) = \begin{cases} 1 & 0 \leq x \leq a \\ 1 - 2 \times \left(\frac{x-a}{c-a}\right)^2 & a \leq x \leq b \\ 2 \times \left(\frac{x-c}{c-a}\right)^2 & b \leq x \leq c \\ 0 & c \leq x \leq L \end{cases} \tag{2}$$

where L is the maximum gray level, $a = 0$, $b = \frac{L}{2}$ and $c = L$. Z -function is used as the fuzzy membership function to denote the degree of homogeneity between two pixels with gray levels $g(i, j)$ and $g(k, l)$, respectively.

Then, based on *fuzzy homogeneity vector*, The *homogram* of an $M \times N$ image is defined as:

$$H(t, d) = \frac{1}{4} \left[\frac{h(t, 0^\circ, d)}{(M-1)N} + \frac{h(t, 45^\circ, d)}{(M-1)(N-1)} + \frac{h(t, 90^\circ, d)}{M(N-1)} + \frac{h(t, 135^\circ, d)}{(M-1)(N-1)} \right] \quad (3)$$

In our experiment $d = 1$, since we want to consider the homogeneity in small regions. [22] discussed how to find the optimal value of d .

2.1.2 Homogram Thresholding

Mode method is one of the widely used techniques for image segmentation [24]. It assumes that images are composed of regions with different gray level ranges, the histogram of an image can be separated into a number of peaks (modes), each corresponds to a region, and there exists a threshold at the valley between any two adjacent peaks. Once the homogram of an image is obtained, the mode method can also be applied to it similarly. The homogram considers both the occurrence of the gray levels and the neighboring homogeneity value among pixels, while histogram-based approaches (HIS) do not take into account any local information. Therefore, homogram thresholding approaches tend to be more effective in finding homogeneous regions than histogram thresholding approaches.

Fuzzy entropy considers the fuzziness of the images based on information theory and fuzzy logic and it is used as a criterion to find thresholds automatically. In [22], the homogram is used to find fuzzy region width and thresholds for segmentation. The modified entropy function under fuzzy set is computed based on the fuzzy region width, Shannon's function and the homogram.

Let $F = \{f_1, f_2, \dots, f_L\}$ be a set of fuzzy membership values which are obtained by fuzzifying all of the gray values in G using the standard S-function and a suitable fuzzy region width; $f_i = \delta_s(g_i)$, where g_i is a gray in G and δ_s is a membership function represented as:

$$\delta_s = S(g, a, b, c) = \begin{cases} 0 & 0 \leq g \leq a \\ 2 \times \left(\frac{g-a}{c-a}\right)^2 & a \leq g \leq b \\ 1 - 2 \times \left(\frac{g-c}{c-a}\right)^2 & b \leq g \leq c \\ 1 & c \leq g \leq L \end{cases} \quad (4)$$

The degree of fuzziness of image I was usually measured by the entropy under fuzzy set F [23]:

$$E(F) = \frac{1}{MN \ln 2} \sum_{x=1}^M \sum_{y=1}^N S_n(\delta_s(g(x, y))) \quad (5)$$

where $S_n(\delta)$ is the Shannon's entropy function. For simplicity, we use δ to represent $\delta_s(g(x, y))$ and $S_n(\delta)$ can be written as:

$$S_n(\delta) = -\delta \ln \delta - (1 - \delta) \ln(1 - \delta) \quad (6)$$

The fuzzy entropy $E(F)$ can also be expressed as:

$$E(F) = \frac{1}{MN \ln 2} \sum_{g=1}^L S_n(\delta_s(g)) f(g) \quad (7)$$

where $f(g)$ denotes the number of occurrences of gray g . It was claimed that the method could sharpen an input histogram by removing the local variations and ambiguities [23]. This premise is not valid for the images where the existent objects cannot be described suitably by the histograms alone; i.e., the spatial dependencies among the pixels have to be considered. Hence, we use $H(g)$ instead of $f(g)/MN$, and redefine the $E(F)$ as:

$$E(F) = \frac{1}{\ln 2} \sum_{g=1}^L S_n(\delta_s(g)) H(g) \quad (8)$$

where $H(g)$ is a homogram denoting the degree of homogeneity of the gray level g . In Eq. 5, $E(F) \in [0, 1]$, indicates the degree of ambiguity of image I .

In our experiment, a is the grey level value corresponding to the leftmost peak of the homogram and c is the grey level value corresponding to the rightmost peak of the homogram. $c - a$ is the width of fuzzy region and $b = \frac{c+a}{2}$.

We apply the fuzzy homogeneity approach to three components of a color image. Then, the segmented results of three components are combined to get all possible clusters.

Assume the range of gray levels of color component i ($i = 1, 2, 3$) is $[L_{i0}, L_{i1}]$, C_i represents the number of thresholds (including L_{i0} and L_{i1}) for color component i , then the set of thresholds for color component i , TS_i , is

$$TS_i = \{T_{i,j} | j = 1, 2, \dots, C_i\}, i = 1, 2, 3 \quad (9)$$

where $T_{i,1} = L_{i0}$ and $T_{i,C_i} = L_{i1}$, and $T_{i,2}, T_{i,3}, \dots, T_{i,C_i-1}$ are the thresholds obtained by the above approach.

Then we can partition the color space into several clusters by

$$\begin{aligned} CLUSTER_{mnl} = & \{(x, y) | g_{I1}(x, y) \in [T_{1,m}, T_{1,m+1}], g_{I2}(x, y) \in [T_{2,n}, T_{2,n+1}] \\ & \text{and } g_{I3}(x, y) \in [T_{3,l}, T_{3,l+1}]\} \end{aligned} \quad (10)$$

where $1 \leq m \leq C_1$, $1 \leq n \leq C_2$, $1 \leq l \leq C_3$, (x, y) is the pixel at row x and column y of a color image, and g_{I1} , g_{I2} and g_{I3} are the three color component images. Each cluster is represented by its average color value.

2.1.3 Color Spaces

Color is perceived by human as a combination of tristimuli R(red), G(green), and B(blue) which are usually called three primary colors. From RGB, we can calculate different kinds of color representations (spaces) by using either linear or nonlinear transformations. Several color spaces, such as RGB, HSI, CIE $L^*u^*v^*$, etc, are employed for color image segmentation, but none of them can dominate the others for all kinds of color images.

Selecting the best color space is still one of the difficulties in color image segmentation [1, 25].

RGB is the most commonly used model for television system and pictures acquired by digital cameras. Video monitors display color images by modulating the intensity of the three primary colors (red, green, and blue) at each pixel of the image [26]. The major disadvantage of RGB and their linear transformations for color scene segmentation and analysis is the high correlation among the R, G, and B components [24, 27]. By high correlation, we mean that if the intensity changes, all the three components will change accordingly.

The HSI (hue-saturation-intensity) system is another commonly used color space in image processing, which is more intuitive to the human vision [28 - 31]. The HSI system separates color information of an image from its intensity information. Color information is represented by hue and saturation values, while intensity, which describes the brightness of an image, is determined by the amount of the light. HSI color space can be described geometrically as in Figure 2 [32]. It is a cylindrical solid. The value range of the hue is from 0° to 360° , the saturation is a radial distance from the cylinder center, and the intensity is the height in the axis direction.

The formulas for hue, saturation, and intensity are:

$$Hue = \arctan\left(\frac{\sqrt{3}(G-B)}{(R-G)+(R-B)}\right)$$

$$Int = \frac{(R+G+B)}{3}$$

$$Sat = 1 - \frac{\min(R,G,B)}{Int}$$

The hue is undefined if the saturation is zero, and the saturation is undefined whenever the intensity is zero. One of the disadvantages of hue is that it has non-removable singularities near the axis of the color cylinder, where a slight change of input R, G, and B values can cause a large jump in the transformed values. The singularities may create discontinuities in the representation of colors [33]. Hue value near its singularities is numerically unstable. That is why pixels having low saturation leave unassigned in

many segmentation algorithms. In addition, if the intensity of the color lies close to white or black, hue and saturation slightly play a role in distinguishing colors.

[34] showed that nonlinear color transformations such as HSI and normalized color space had essential singularities which were non-removable, and there were spurious modes in the distribution of values resulting from the nonlinear transformations. [34] suggested that linear spaces, such as YIQ, be used, rather than nonlinear spaces. The major problem of linear color spaces is the high correlation of the three components, which makes the three components dependent upon each other and associate strongly with intensity. Hence, linear spaces are very difficult to discriminate highlights, shadows and shading in color images. Besides, if a linear color space is used, image segmentation has to be performed in a 3D space, usually on one component a time, because it is difficult to combine the information inherent in these components. However, nonlinear color spaces do not have such problems. In HSI space, hue can be used for segmentation when the saturation is not low, and certain types of highlights, shadows and shading can be discounted [21].

2.2 The Region Merging Approach

At the first stage, finding all major classes is essential to the final segmentation. Therefore, we have to select proper parameters for determining “peaks” of the homogram and fuzzy entropy of the image at the first stage. This might lead to oversegmentation, i.e., homogeneous regions with narrow color transition might be split as separate regions, or very small regions might be generated. Hence, the clusters achieved at the first stage are not the final segmentation results. Some of these clusters may contain very few pixels and should not be considered as proper clusters. Also there might be some clusters that are very close to each other and they may need to be combined. We use the region merging approach to solve this problem.

2.2.1 The Region Merging Criterion

One problem with region merging is how to define merging criteria. Incorporating specific knowledge of psychophysical perception is an ideal way, but this is not practical for application. Generally, region merging is based on both feature space and the spatial relation between pixels simultaneously. In this paper, the definition of a region is based on similar color. Hence, we only take into account color similarity when deciding if two regions are to be merged.

We select RGB as the color space to measure the distance between two clusters C_m and C_n :

$$Dist(C_m, C_n) = max(|R_m - R_n|, |G_m - G_n|, |B_m - B_n|) \quad (11)$$

where (R_m, G_m, B_m) and (R_n, G_n, B_n) are the average color values of cluster C_m and cluster C_n .

2.2.2 Region Merging Strategy

Another problem with region merging is that the final segmentation is dependent on the order in which regions are examined. The strategy in our method is: First, each cluster whose number of pixels is less than a predefined threshold is merged into its closest cluster until no such clusters exist; then region merging is performed iteratively by combining the two closest regions each time until the distances of all the pairs of regions are greater than a specified global threshold. The algorithm for the region merging process is described as follows:

Begin /* Region Merging Process */

/* Merge those clusters with quite few pixels into their closest clusters */

$M :=$ the number of all clusters;

$setOfInvalidCluster :=$ all those clusters whose numbers of pixels are less than N_s ;

While $setOfInvalidCluster$ is not EMPTY do {

```

Find two clusters  $C_s$  and  $C_t$  satisfying:
 $Dist(C_s, C_t) = \min \{Dist(C_i, C_j) \mid 1 \leq i, j \leq M \text{ and at least one of } C_i \text{ and } C_j$ 
belongs to setOfInvalidCluster};

Merge  $C_s$  and  $C_t$  into a new cluster  $C_k$ ;
M := M - 1;
If the number of pixels of cluster  $C_k < N_0$ 
Then Add cluster  $C_k$  to setOfInvalidCluster
}

/* Merge those closest pairs of clusters */
Find two clusters  $C_s$  and  $C_t$  satisfying:  $Dist(C_s, C_t) = \min \{Dist(C_i, C_j) \mid 1 \leq i, j \leq M\}$ ;
While  $Dist(C_s, C_t) < D_s$  do {
Merge  $C_s$  and  $C_t$  into a new cluster  $C_k$ ;
M := M - 1;
Find two clusters  $C_s$  and  $C_t$  satisfying:  $Dist(C_s, C_t) = \min \{Dist(C_i, C_j) \mid 1 \leq i, j \leq M\}$ ;
}
End /* Region Merging Process */

```

N_s is the threshold for number of pixels in a cluster and D_s is the threshold for the distance between two clusters. According to our experiments on more than 100 images, $N_s = 10$ and $D_s = 20$ are more appropriate.

3 EXPERIMENT AND DISCUSSION

We have done experiments on a variety of images to test the proposed approach. We applied the proposed approach to both RGB and HSI color spaces, and compared the results with those obtained by using the histogram-based approach.

3.1 Homogram vs. Histogram

Figures 3 - 6 show the experimental results using RGB color space. Histogram-based approach (HIB) is similar to the homogram-based approach (HOB) except the first one use histogram to segment the image. Table 1 and Table 2 list the results of Figs. 4-6 using the HOB and HIB approaches with RGB representations, respectively.

The original image, BUTTERFLY, is shown in Fig. 3(a). The entropies of its R, G and B components by the HOB are shown in Fig. 3(b), Fig. 3(c) and Fig. 3(d), and the entropies of its R, G and B components by the HIB are shown in Fig. 3(e), Fig. 3(f) and Fig. 3(g), respectively. Fig. 3(h) and Fig. 3(i) are the resulting images by HOB, after the first stage and second stage, and Fig. 3(j) and Fig. 3(k) are the resulting images by the HIB after the first stage and second stage, respectively. In Fig. 3(h), the wings of the butterfly are clearly and homogeneously segmented, while in Fig. 3(j), some areas on the upper left side and below the butterfly are assigned the same color as the wings. The numbers of clusters generated by HOB and HIB are 74 and 72, respectively. Fig. 3(i) is the result after merging operation on Fig. 3(h), and only 23 regions are left, but the effect is still very good because main features are not affected.

Figs. 4-6 are three more images selected to show the comparison between the two segmentation approaches. In Fig. 4(h), the resulting image by the HOB, good effects are achieved, while in Fig. 4(j), the resulting image by the HIB, we can see that the body of the frog, the lower left corner of the image and the green triangle on the upper right side are not properly segmented, The numbers of clusters generated by HOB and HIB are 40 and 33, respectively. Fig. 4(i) is the resulting image after merging operation on Fig. 4(h) with fewer and much more homogeneous segments.

Fig. 5(h) is much better than Fig. 5(j). In Fig. 5(j), the green beans, the yellow beans and the background are incorrectly segmented, and many green beans are totally lost. We can also notice that Fig. 5(i), the result after merging of Fig. 5(h), still has good visual effect with only 14 clusters, while Fig. 5(h) has 30 clusters.

Fig. 6(h), is much clearer than Fig. 6(j). The hair and skin of the girl and the background are not correctly segmented in Fig. 6(j), whereas they have no problems in Fig. 6(h). The number of clusters is greatly reduced from 80 to 16 by the merging process.

Figures 7 - 10 show the results obtained using HSI color space, and the results of segmentation are listed in Tables 3 and 4 for HOB and HIB, respectively.

In Fig. 7, the original image, RFLR, is shown in Fig. 7(a). The entropies of its H, S and I components by the HOB are shown in Fig. 7(b), Fig. 7(c) and Fig. 7(d), and the entropies of its H, S and I components by the HIB are shown in Fig. 7(e), Fig. 7(f) and Fig. 7(g), respectively. Fig. 7(h) and Fig. 7(i) are the resulting images by the HOB, after the first stage and second stage, and Fig. 7(j) and Fig. 7(k) are the resulting images by the HIB, after the first stage and second stage, respectively. It is obvious that Fig. 7(h) is much more clearly and homogeneously segmented than Fig. 7(j). In Fig. 7(j), the red parts and blue background are wrongly segmented. Fig. 7(i) is the result after merging of Fig. 7(h). Many isolated pixels and small clusters are merged into their closest clusters, so the number of clusters are reduced from 28 to 12. The image after merging has more homogeneous background and is more clear than that before merging.

In Fig. 8, the hair and face of the girl are better extracted in the resulting images by the HOB (Fig. 8(c)) than that by the HIB (Fig. 8(e)). Fig. 9(c) is much closer to the original image than Fig. 9(e). Many yellow areas in the original image are lost in the resulting image by the HIB. Finally, in Fig. 10, we can easily see that the resulting image by the HOB is much clearer and more homogeneous than that by the HIB. In Fig. 10(b), the green stem, the violet flower and the yellow background are clearly extracted, and after merging, the resulting regions are more homogeneous than that before merging (see Fig. 10(c)), while in Fig. 10(d), all these regions are mixed up.

As we can figure out from the experimental results, the HOB works better than the HIB. The reason is that while the entropies are computed, the HOB considers both

global and local information of an image, while HIB does not take into account the spatial dependencies among pixels.

3.2 RGB vs. HSI

Non-removable singularity is one of hue’s drawbacks that may create discontinuities and spurious modes in the representation of colors [33]. In an image with low saturation, hue value near its singularity is numerically unstable, which makes homogeneity defined by Eq. (1) unreliable. However, hue can be used to extract colors in a color image with high saturation, and may achieve better effects than RGB color space where the three components are highly correlated. Here we select three images, GIRL (Fig. 8(a)), TREE (Fig. 9(a)) and VFLR (Fig. 10(a)) to illustrate such nature.

The proposed method is applied to these images in both RGB and HSI spaces. The results of segmentation are listed in Table 3 and Table 5 for HSI and RGB, respectively.

Fig. 11(b) is the resulting image by the HOB method using RGB color space. The color of the skin and the lower part of the green clothes are not correctly extracted. In Fig. 12(b), the orange color over the upper right part is not properly segmented, even though the number of clusters at first stage is 94. The number of clusters in Fig. 9(c) is only 53, but its effect is better than that in Fig. 12(a) because main features can be remained. Fig. 13 can also show the advantage of HSI over RGB. In Fig. 10(c), the green stem, the violet flower and the yellow background are clearly segmented, while in Fig. 13(a), these colors are incorrectly segmented. Though these two approaches may have similar number of clusters, the results using the HOB with RGB color space are worse than using HSI due to the correlation among the color components.

4 CONCLUSIONS

We have presented a color image segmentation approach based on homogram thresholding and region merging. The key point of this approach is that homogram analysis is used to extract all major homogeneous regions at the first stage and the region merging process is performed iteratively based on color similarity among these regions to solve the problem of oversegmentation. The experimental results show that the HOB tends to be more effective to find homogeneous regions and to extract the homogeneous regions with gradual shading in color images than HIB does.

The proposed approach operates in RGB and HSI color spaces for comparison. The non-removable singularity of hue may create spurious modes in the distribution of values resulting from the nonlinear transformations, which makes the homogram of hue value unreliable for segmentation. RGB color space does not have such a problem. But for a color image with high saturation, segmentation using HSI can generate very good results, even better than that using RGB. The reason is that the three components R, G and B have high correlation which makes the three components depend on each other and associate strongly with intensity.

References

- [1] H. D. Cheng, X. H. Jiang, Ying Sun and Jingli Wang, "Color Image Segmentation: Advances and Prospects," To appear in *Pattern Recognition*, 2001.
- [2] C. K. Yang and W. H. Tsai, "Reduction of Color Space Dimensionality by Moment-preserving Thresholding and Its Application for Edge Detection in Color Images," *Pattern Recognition Letters*, Vol. 17, 481-490, 1996.
- [3] Y. Ohta, T. Kanade and T. Sakai, "Color Information for Region Segmentation," *Computer Graphics and Image Processing*, Vol. 13, 222-241, 1980.
- [4] D. Tseng and C. H. Chang, "Color Segmentation Using Perceptual Attributes," *IEEE International Conference on Image Processing-A*, 228- 231, 1992.
- [5] R. Ohlander, K. Price and D. R. Reddy, "Picture Segmentation Using A Recursive Region Splitting Method," *Computer Graphics and Image Processing*, 8, 313-333, 1978.
- [6] S. Tominaga, "Color Image Segmentation Using Three Perceptual Attributes," *Proceedings of the Conference Vision and Pattern Recognition, IEEE Computer Society*, Los Alamitos, CA, 628-630, 1986.
- [7] M. Celenk, "A Color Clustering Technique for Image Segmentation," *Graphical Models and Image Processing*, Vol. 52, No. 3, 145-170, 1990.
- [8] N. Ito, et al., "The Combination of Edge Detection and Region Extraction in Non-parametric Color Image Segmentation," *Information Sciences*, 92, 277-294, 1996.
- [9] Y. Xiaohan and J. Yla, "Image Segmentation Combining Region Growing with Edge Detection," *11th IAPR Int. Conf. Pattern Recognition, Image, Speed, and Signal Analysis*, The Netherlands, 481-484, 30 August-3 September 1992.

- [10] T. Pavlidis and Y. T. Liow, "Integrating Region Growing and Edge Detection," *IEEE Trans. Pattern Anal. Machine Intell.*, 12(3): 225-233, 1990.
- [11] Q. Huang, et al., "Foreground/Background Segmentation of Color Images by Integration of Multiple Cues," *IEEE International Conference on Image Processing-A*, 246-249, 1995.
- [12] Q. Huang, B. Dom, N. Megiddo and W. Niblack, "Segmenting and Representing Background in Color Images," *International Conference on Image Processing-C*, 13-17, 1996.
- [13] R. I. Taylor and P. H. Lewis, "Color Image Segmentation Using Boundary Relaxation," *IEEE International Conference on Image Processing-C*, 721-724, 1992.
- [14] R. Schettini, "A Segmentation Algorithm for Color Images," *Pattern Recognition Letter*, 14, 499-506, 1993.
- [15] S. K. Pal, et al., "A Review on Image Segmentation Techniques," *Pattern Recognition*, 29, 1277-1294, 1993.
- [16] K. S. Fu and J. K. Mui, "A Survey on Image Segmentation," *Pattern Recognition*, 13, 3-16, 1981.
- [17] R. M. Haralick and L.G. Shapiro, "Image Segmentation Techniques," *Computer Vision, Graphics and Image Processing*, 29, 100-132, 1985.
- [18] P. K. Sahoo, et. al, "A Survey of Thresholding Techniques," *Computer Vision, Graphics and Image Processing*, 41, 233-260, 1988.
- [19] L. Spirkovska, "A Summary of Image Segmentation Techniques," *NASA Technical Memorandum 104022*, June 1993.

- [20] C. H. Chen, "On the Statistical Image Segmentation Techniques," *Proceedings, IEEE Conference Pattern Recognition and Image Processing*, 262-266, 1981.
- [21] P. W. M. Tsang and W. H. Tsang, "Edge Detection on Object Color," *IEEE International Conference on Image Processing-C*, 1049-1052, 1996.
- [22] H. D. Cheng, C. H. Chen, H. H. Chiu and H. J. Xu, "Fuzzy Homogeneity Approach to Multilevel Thresholding," *IEEE Transactions on Image Processing*, Vol. 7, No. 7, 1-5, July 1998.
- [23] S. K. Pal and D. K. D. Majumder, *Fuzzy Mathematical Approach to Pattern Recognition*, NY: John Wiley & Sons, 1986.
- [24] E. Littmann and H. Ritter, "Adaptive Color Segmentation - A Comparison of Neural and Statistical Methods," *IEEE Transactions on Neural Network*, Vol. 8, No. 1, 175- 185, 1997.
- [25] J. Gauch and C. W. Hsia, "A Comparison of Three Color Image Segmentation Algorithm in Four Color Spaces," *SPIE Vol. 1818 Visual Communications and Image Processing '92*, 1168 -1181, 1992.
- [26] M. T. Orchard and C. A. Bouman, "Color Quantization of Images," *IEEE Transactions on Signal Processing*, Vol. 39, No. 12, 2677-2690, December 1991.
- [27] M. Pietikainen, et al., "Accurate Color Discrimination with Classification Based on Feature Distributions," *International Conference on Image Processing-C*, 833-838, 1996.
- [28] T. L. Huntsberger, C. L. Jacobs and R. L. Cannon, "Iterative Fuzzy Image Segmentation," *Pattern Recognition*, Vol. 18, No. 2, 131-138, 1985.

- [29] T. Carron and P. Lambert, "Color Edge Detector Using Jointly Hue, Saturation and Intensity," *International Conference on Image Processing 94*, Austin, USA, 977-081, 1994.
- [30] Y. Rui, A. C. She and T. S. Huang, "Automated Region Segmentation Using Attraction-based Grouping in Spatial-color-texture space," *International Conference on Image Processing-A*, 53-56, 1996.
- [31] W. S. Kim and R. H. Park, "Color Image Palette Construction Based on the HSI Color System for Minimizing the Reconstruction Error," *IEEE, International Conference on Image Processing-C*, 1041-1044, 1996.
- [32] D. E. P. Hoy, "On the Use of Color Imaging in Experimental Applications," *Experimental Techniques*, July/August, 17-19, 1997.
- [33] M. Chapron, "A new Chromatic Edge Detector Used for Color Image Segmentation," *IEEE International Conference on Image Processing-A*, 311- 314, 1992.
- [34] J. Kender, "Saturation, Hue, and Normalized Color: Calculation, Digitization Effects, and Use," *Computer Science Technical Report*, Carnegie Mellon University, 1976.

Table 1: Results of the HOB using RGB Color Space

Name of Image	# of segments			# of clusters	
	R	G	B	before merging	after merging
BUTTERFLY	5	10	3	74	23
FROG	3	4	5	40	18
JELLY_BEANS	3	6	3	30	14
LIZI	8	8	4	84	16

Table 2: Results of the HIB using RGB Color Space

Name of Image	# of segments			# of clusters	
	R	G	B	before merging	after merging
BUTTERFLY	4	8	5	72	21
FROG	3	3	5	33	12
JELLY_BEANS	3	4	3	22	9
LIZI	5	6	4	40	14

Table 3: Results of the HOB using HSI Color Space

Name of Image	# of segments			# of clusters	
	H	S	I	before merging	after merging
RFLR	5	2	5	36	14
GIRL	17	4	7	166	12
TREE	3	4	6	53	22
VFLR	3	4	4	33	10

Table 4: Results of the HIB using HSI Color Space

Name of Image	# of segments			# of clusters	
	H	S	I	before merging	after merging
RFLR	5	2	4	28	12
GIRL	16	6	5	131	11
TREE	3	4	4	33	13
VFLR	3	3	3	22	9

Table 5: Results of the HOB using RGB Color Space

Name of Image	# of segments			# of clusters	
	R	G	B	before merging	after merging
GIRL	8	6	6	53	11
TREE	3	4	17	94	25
VFLR	3	3	2	14	7

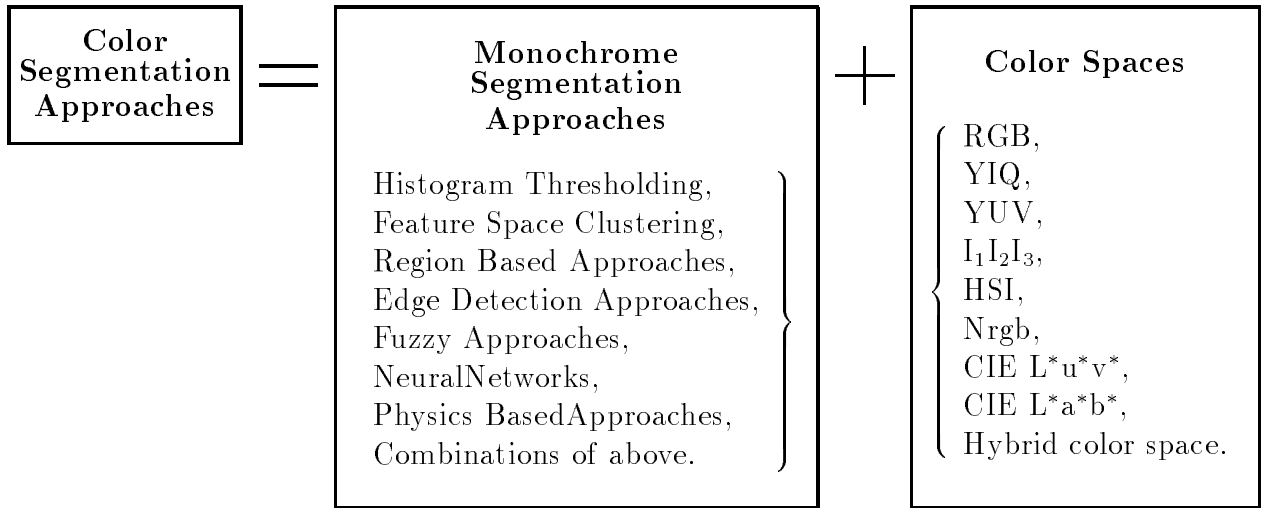


Figure 1. Commonly used color image segmentation approaches [1]

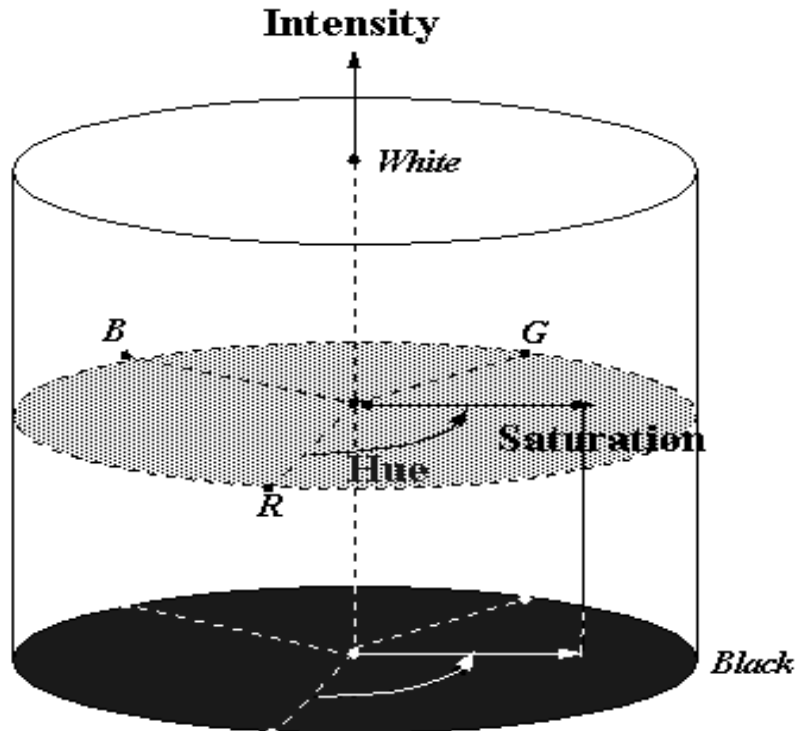
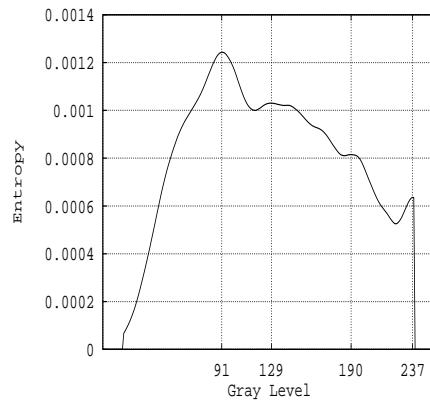


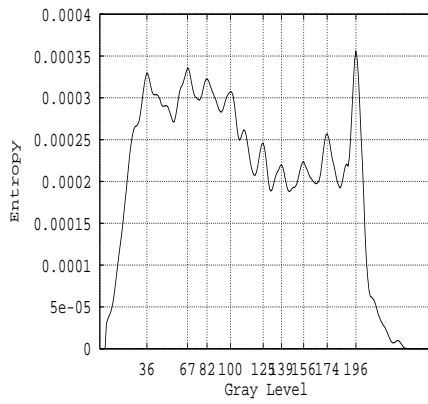
Figure 2: HSI color space [32]



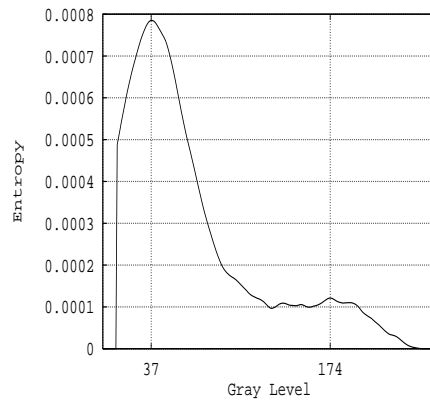
(a)



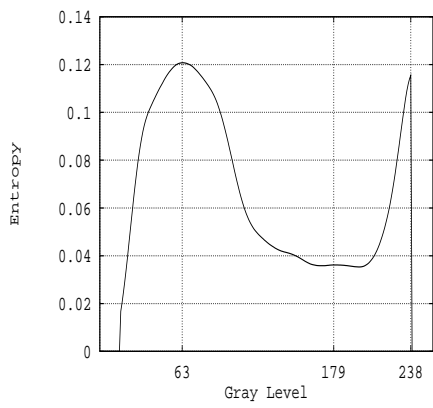
(b)



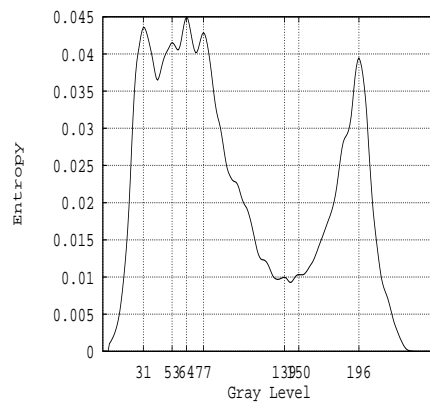
(c)



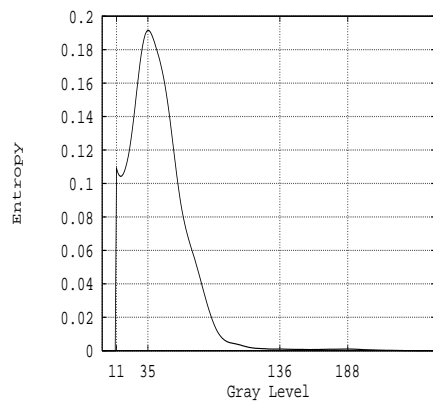
(d)



(e)



(f)



(g)

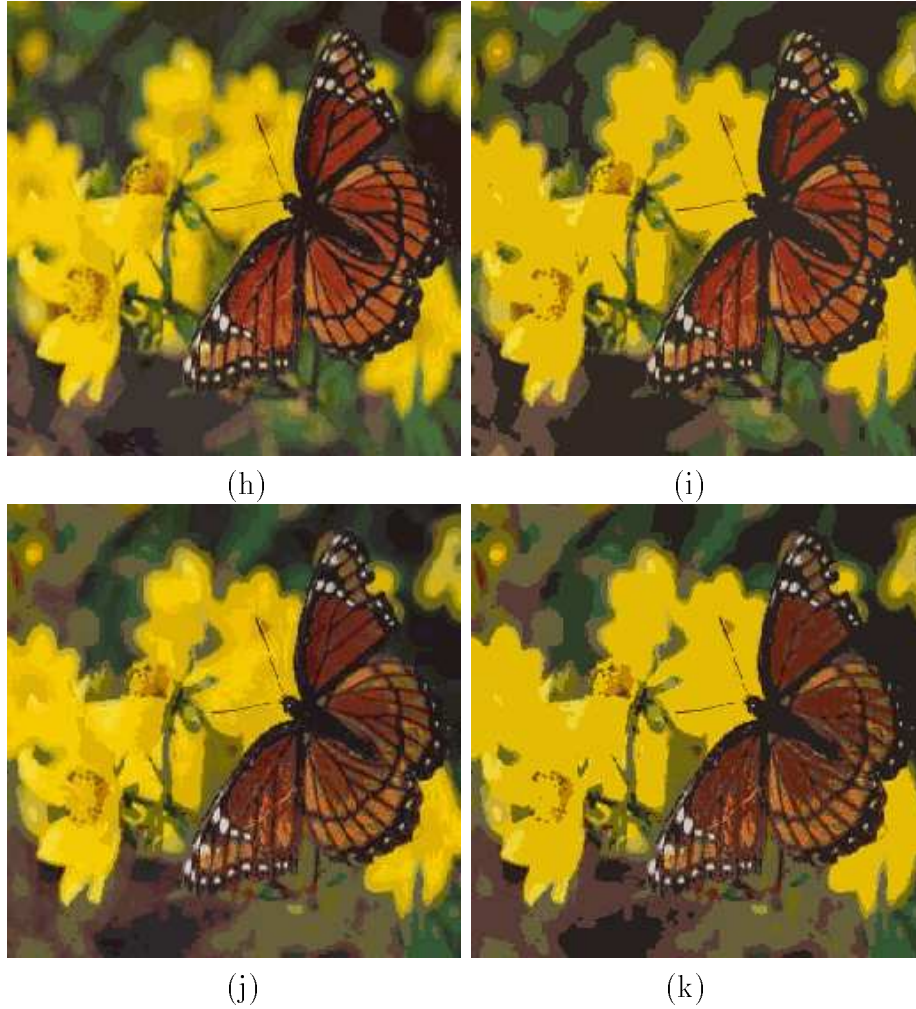
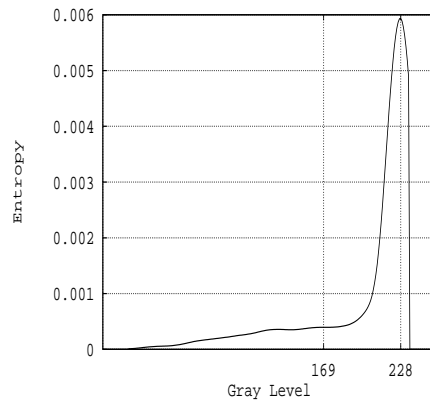


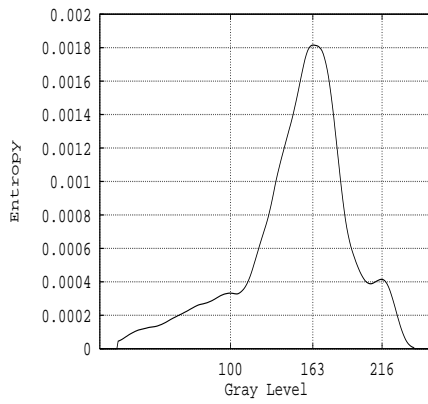
Figure 3: (a) The original image BUTTERFLY. (b) R's entropy by HOB. (c) G's entropy by HOB. (d) B's entropy by HOB. (e) R's entropy by HIB. (f) G's entropy by HIB. (g) B's entropy by HIB. (h) Result after the first stage of the HOB (i) Final result of the HOB. (j) Result after the first stage of HIB. (k) Final result of the HIB.



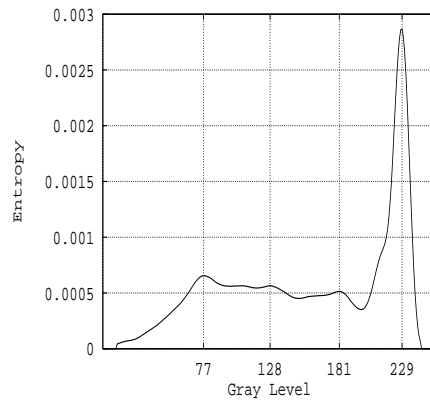
(a)



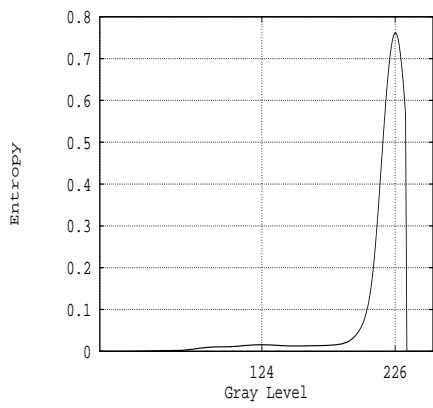
(b)



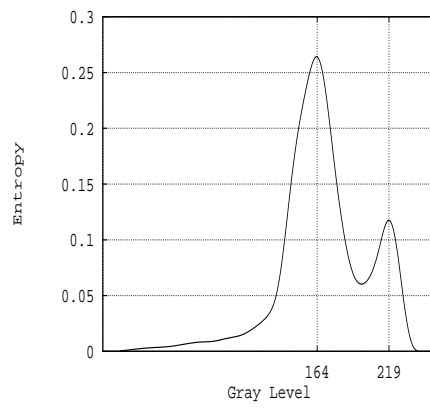
(c)



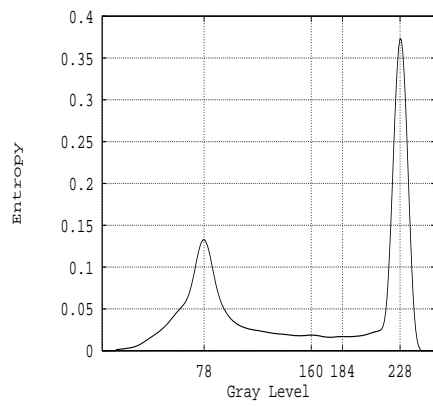
(d)



(e)



(f)



(g)

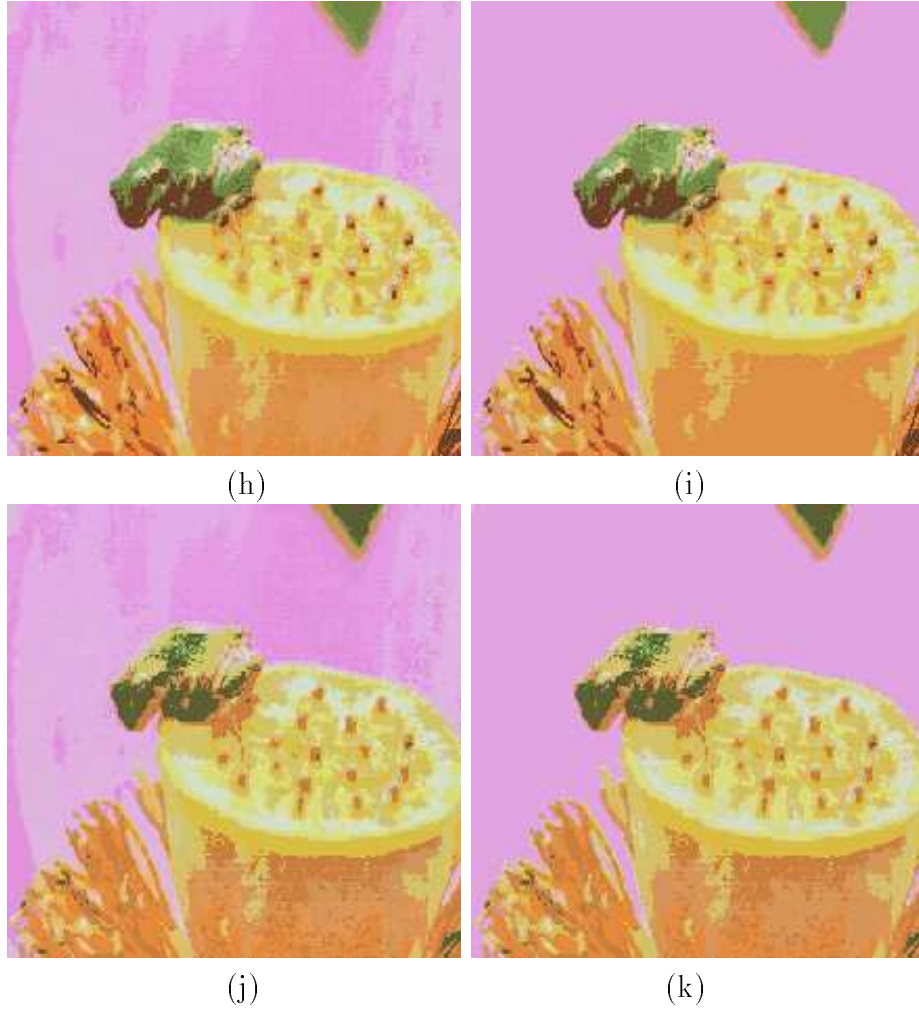
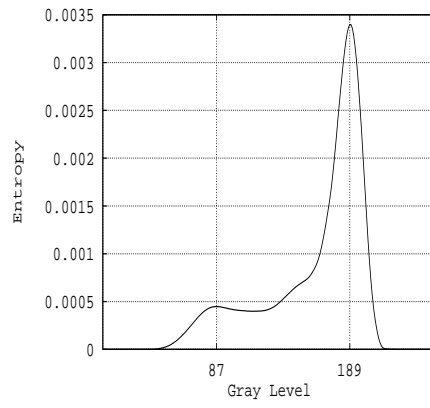


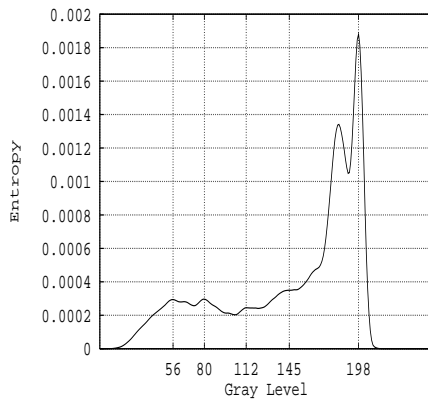
Figure 4: (a) The original image FROG. (b) R's entropy by HOB. (c) G's entropy by HOB. (d) B's entropy by HOB. (e) R's entropy by HIB. (f) G's entropy by HIB. (g) B's entropy by HIB. (h) Result after the first stage of the HOB (i) Final result of the HOB. (j) Result after the first stage of HIB. (k) Final result of the HIB.



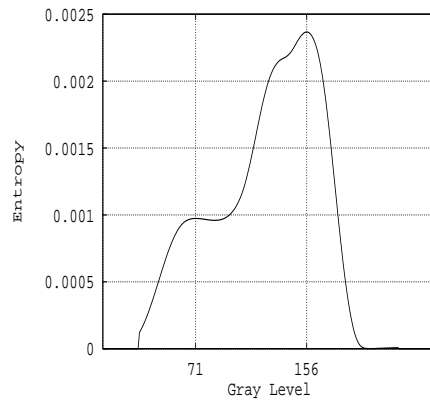
(a)



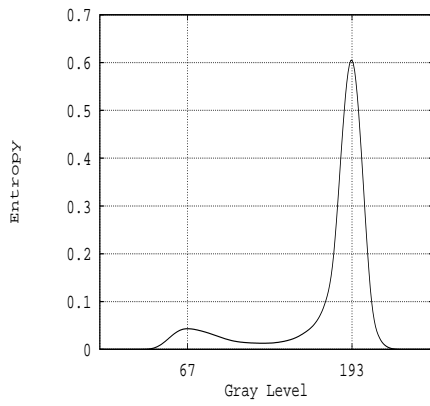
(b)



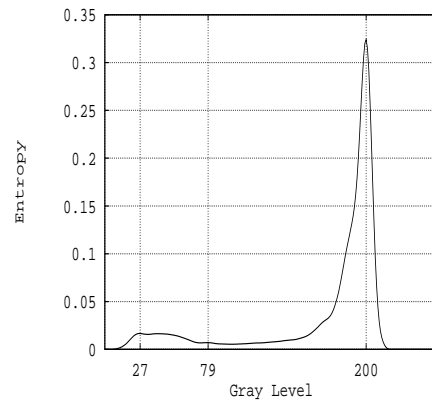
(c)



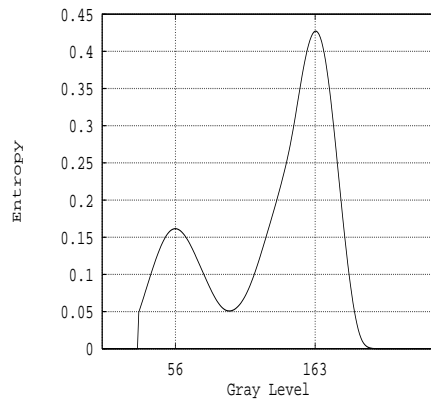
(d)



(e)



(f)



(g)

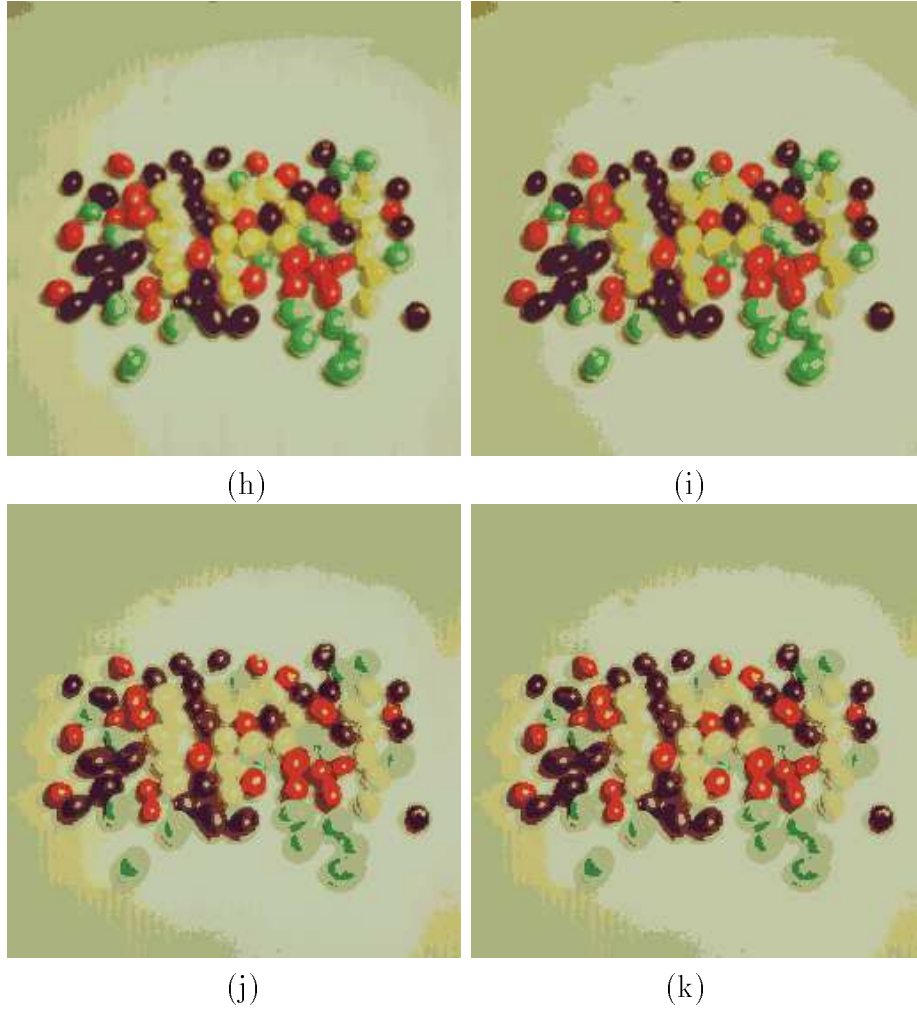
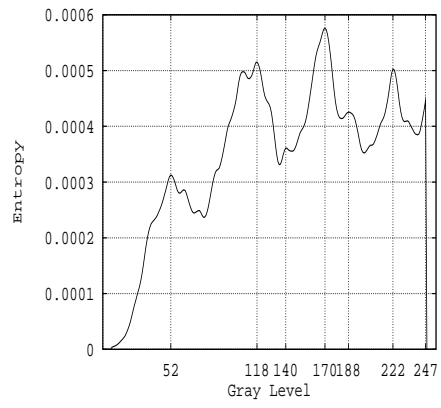


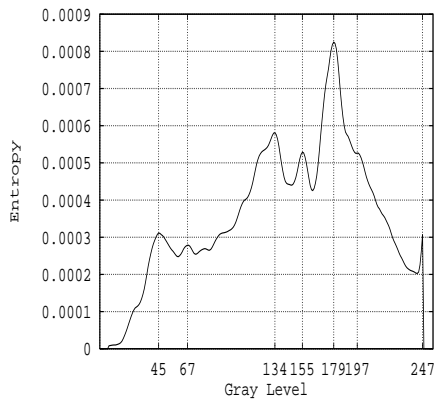
Figure 5: (a) The original image JELLYBEANS. (b) R's entropy by HOB. (c) G's entropy by HOB. (d) B's entropy by HOB. (e) R's entropy by HIB. (f) G's entropy by HIB. (g) B's entropy by HIB. (h) Result after the first stage of the HOB (i) Final result of the HOB. (j) Result after the first stage of HIB. (k) Final result of the HIB.



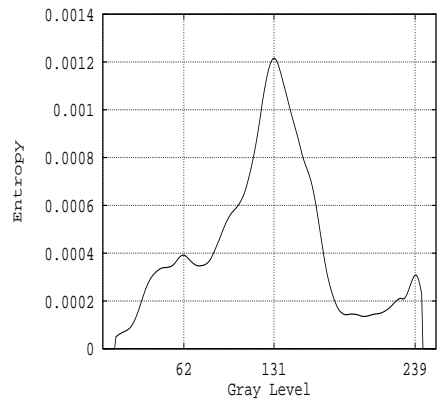
(a)



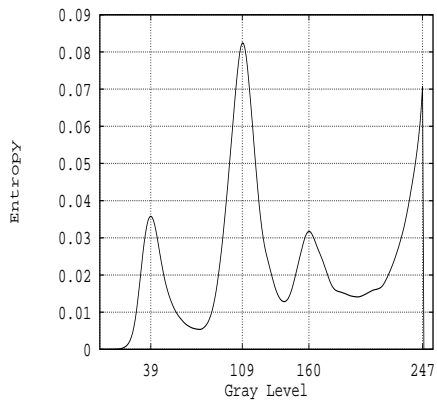
(b)



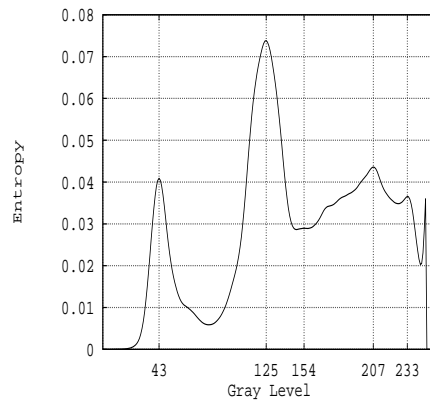
(c)



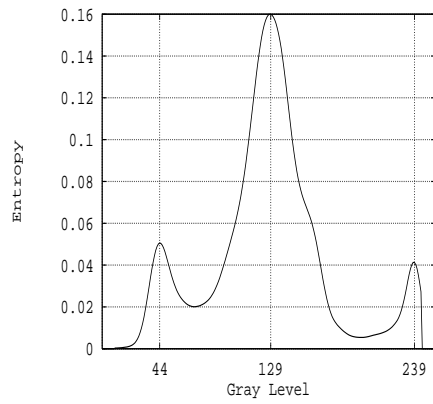
(d)



(e)



(f)



(g)

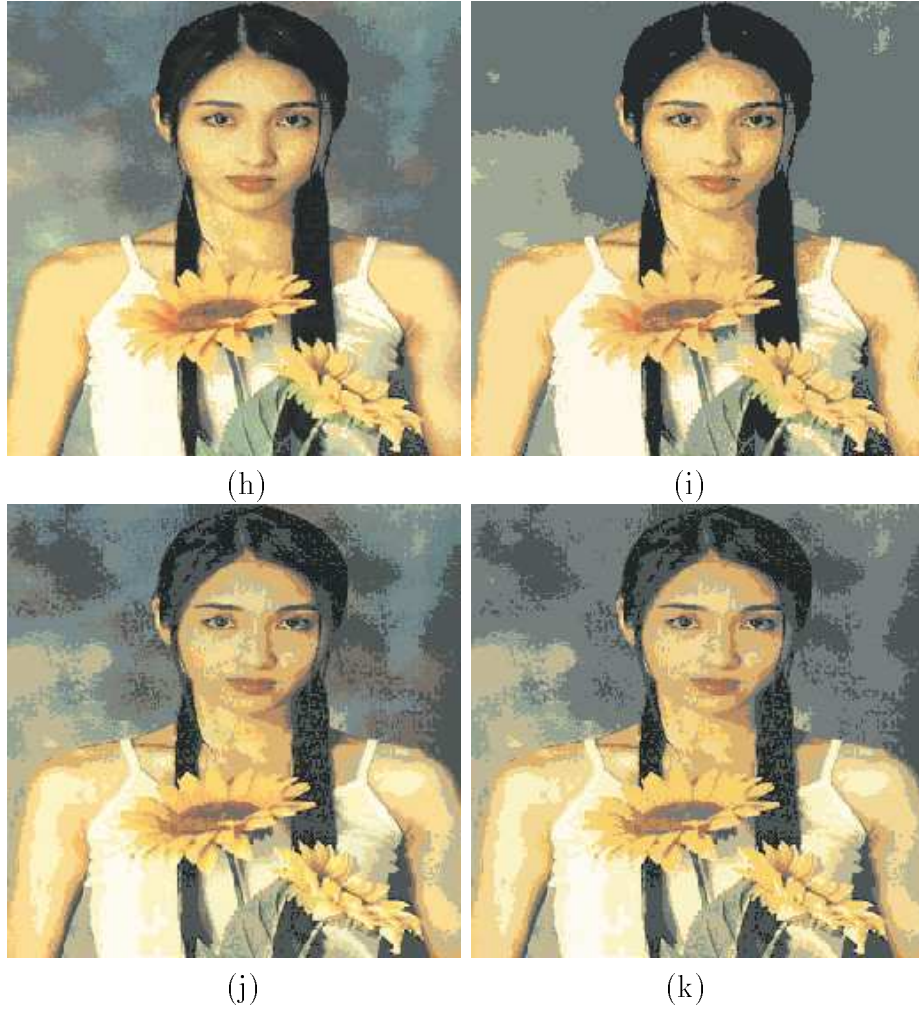
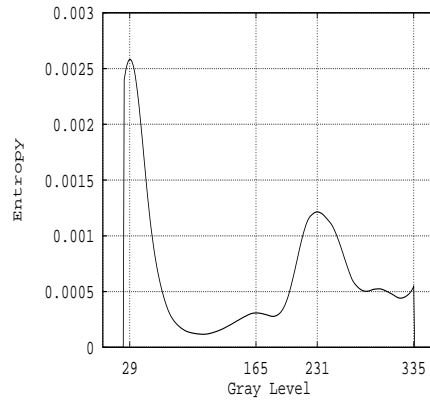


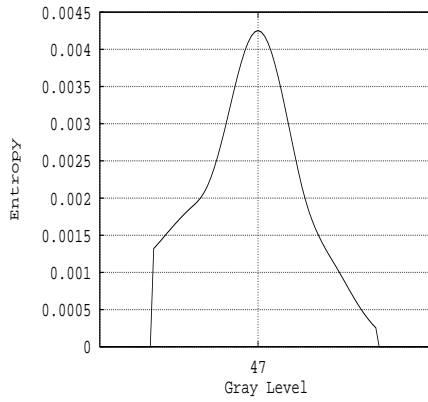
Figure 6: (a) The original image LIZI. (b) R's entropy by HOB. (c) G's entropy by HOB. (d) B's entropy by HOB. (e) R's entropy by HIB. (f) G's entropy by HIB. (g) B's entropy by HIB. (h) Result after the first stage of the HOB (i) Final result of the HOB. (j) Result after the first stage of HIB. (k) Final result of the HIB.



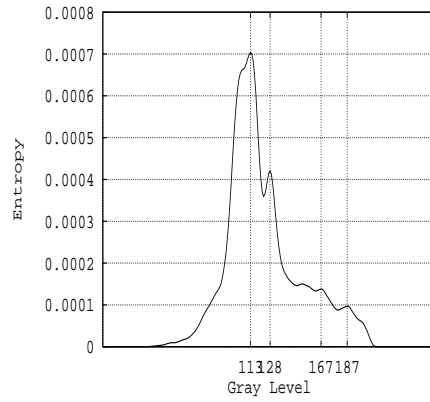
(a)



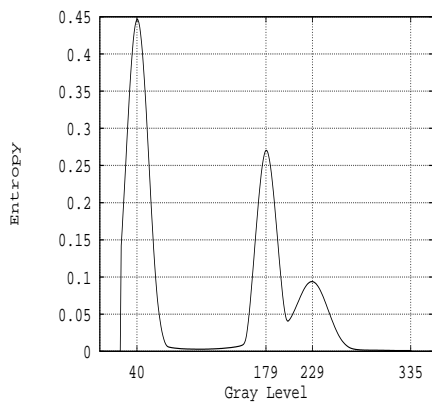
(b)



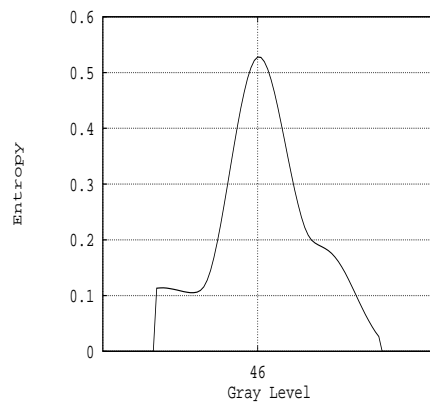
(c)



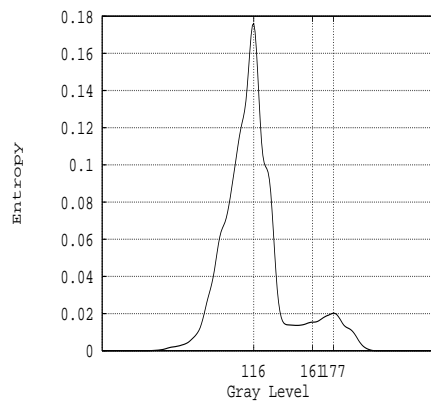
(d)



(e)



(f)



(g)

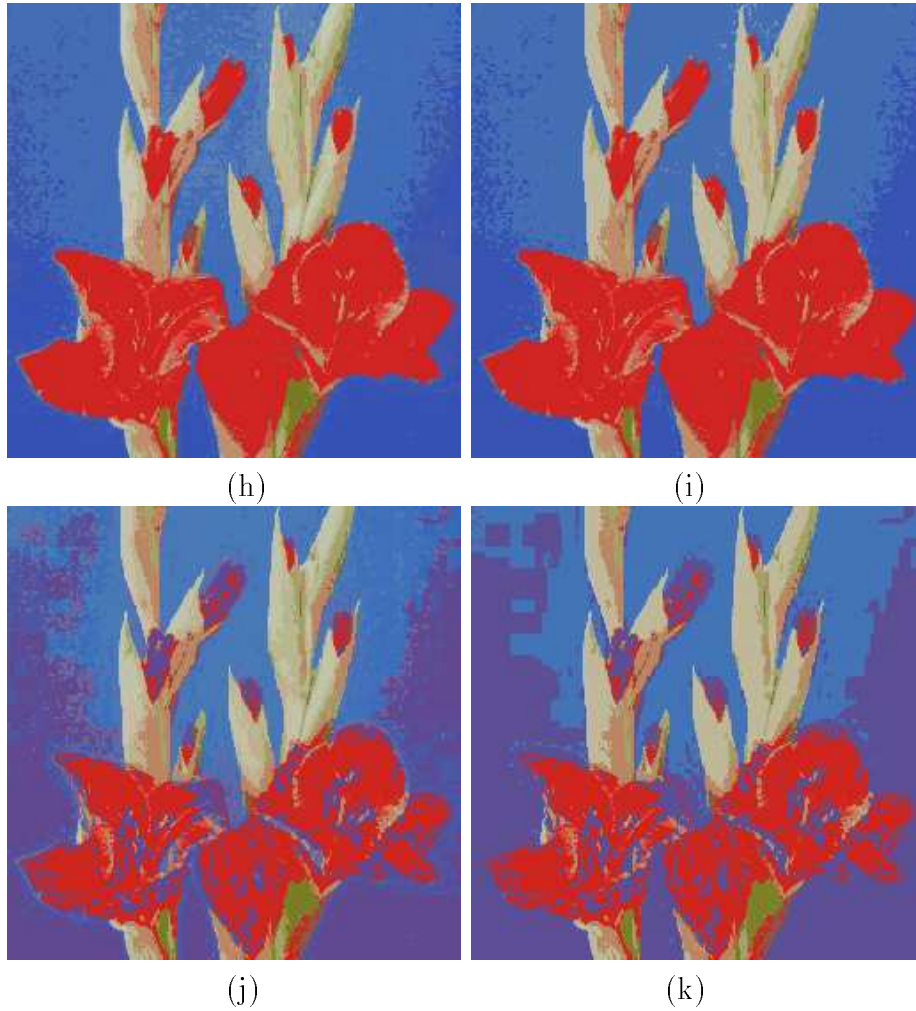


Figure 7: (a) The original image RFLR. (b) H's entropy by HOB. (c) S's entropy by HOB. (d) I's entropy by HOB. (e) H's entropy by HIB. (f) S's entropy by HIB. (g) I's entropy by HIB. (h) Result after the first stage of the HOB (i) Final result of the HOB. (j) Result after the first stage of HIB. (k) Final result of the HIB.